ACS Partner Journal

Journal of the American Society for Mass Spectrometry

pubs.acs.org/jasms

Research Article

Ion Mobility and Fourier Transform Ion Cyclotron Resonance Collision Cross Section Techniques Yield Long-Range and Hard-Sphere Results, Respectively

Tina Heravi, Andrew J. Arslanian, Spencer D. Johnson, and David V. Dearden*

Cite This: *J. Am. Soc. Mass Spectrom.* 2022, 33, 1644−1652

Read Online

ACCESS | Metrics & More | Article Recommendations | Supporting Information

ABSTRACT: We determined collision cross section (CCS) values for singly and doubly charged cucurbit[*n*]uril (*n* = 5−7), decamethylcucurbit[5]uril, and cyclohexanocucurbit[5]uril complexes of alkali metal cations (Li^+−Cs^+). These hosts are relatively rigid. CCS values calculated using the projection approximation (PA) for computationally modeled structures of a given host are nearly identical for +1 and +2 complexes, with weak metal ion dependence, whereas trajectory method (TM) calculations of CCS for the same structures consistently yield values 7−10% larger for the +2 complexes than for the corresponding +1 complexes and little metal ion dependence. Experimentally, we measured relative CCS values in SF_6 for pairs of +1 and +2 complexes of the cucurbituril hosts using the cross-sectional areas by Fourier transform ion cyclotron resonance ("CRAFTI") method. At center-of-mass collision energies <∼30 eV, CRAFTI CCS values are sensitive to the relative binding energies in the +1 and +2 complexes, but at collision energies >∼40 eV (sufficient that ion decoherence occurs on essentially every collision) that dependence is not evident. Consistent with the PA calculations, these experiments found that the +2 complex ions have CCS values ranging between 94 and 105% of those of their +1 counterparts (increasing with metal ion size). In contrast, but consistent with the TM CCS calculations, ion mobility measurements of the same complexes at close to thermal energies in much less polarizable N_2 find the CCS of +2 complexes to be in all cases 9−12% larger than those of the corresponding +1 complexes, with little metal ion dependence.

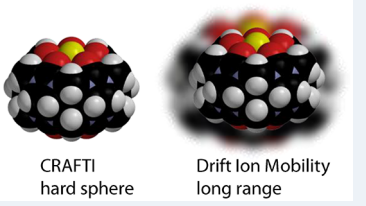

INTRODUCTION

Collision cross section (CCS) measurements have recently seen a dramatic increase in popularity and importance[1] because cross section measurements give information about molecular conformation while requiring only small amounts of material. For example, cross section measurements can often distinguish between isomers that would otherwise appear identical in a mass spectrum. For supramolecular complexes, cross section data are useful for structure elucidation; externally and internally bound guests in host−guest complexes often yield distinguishably different CCS values.[2−4]

The most common method for measuring CCS in the gas phase is ion mobility coupled with mass spectrometry (IM-MS), especially for characterizing peptide and protein conformations.[5] In a conventional drift tube ion mobility instrument, ions travel through a uniform electric field in the presence of a buffer gas. IM-MS experiments inherently involve multiple low-energy collisions with the neutral buffer gas. The proportionality constant between the drift velocity of the ions and the electric field is the ion mobility and is dependent on the collision integral between the ion and the buffer gas. Larger ions undergo more collisions with the buffer gas compared to smaller ions and thus have lower mobilities, other things being equal.[6] It should be noted that IM-MS directly measures mobilities, which can be related to collision integrals (and less directly) to CCS via the Mason−Schamp equation.[7] Long-range interactions between the ion and the buffer gas can affect the conformations of the ions[8,9] and influence CCS values at low collision energies.[10]

A more recent method involves measuring CCS using techniques from Fourier transform ion cyclotron resonance mass spectrometry (FTICR-MS). We refer to this method as CRAFTI (an acronym for *cr*oss sectional *a*reas by *F*ourier *t*ransform *i*on cyclotron resonance mass spectrometry).[11−13] CRAFTI obtains ion-neutral collision cross sections from the pressure-limited rate of signal decay, reflected in the ion line widths in Fourier transform mass spectra. Thus, both CCS and the mass-to-charge ratio can be measured at the same time using one instrument. The CRAFTI technique importantly differs from drift IM-MS in that most of the CRAFTI experiment is conducted under high vacuum conditions. As a result, ion−molecule collisions are minimized prior to the CCS measurement. The pressure of a neutral collision gas is temporarily increased for the detection event of the experiment to ensure that the ions decohere from a coherently orbiting

Received: April 19, 2022
Revised: July 12, 2022
Accepted: August 8, 2022
Published: August 12, 2022

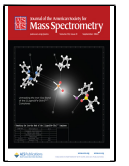

https://doi.org/10.1021/jasms.2c00112
J. Am. Soc. Mass Spectrom. 2022, 33, 1644−1652

packet primarily via single ion-neutral collisions at relatively high kinetic energy. This can enable measurement of collision cross sections for collisionally labile complexes that are difficult to measure in the collision-rich environment of drift IM-MS.[14]

Earlier work has shown that collision-induced dissociation (CID) is a primary means of decoherence in CRAFTI.[11] This leads to a concern that complexes that dissociate easily might therefore yield larger cross sections than complexes of the same physical size that are more strongly bound. As long as single collisions always decohere the ions (and dissociation always results in decoherence, because it changes the cyclotron frequency of the resulting fragment ion) this would not be a problem. However, CRAFTI measurements of higher m/z ions can be problematic if the center-of-mass collision energies required for single-collision CID cannot be reached prior to ejecting the ions from the trapping cell. One way of addressing this problem is to apply the technique to ions that can dissociate at lower energies. Because they are relatively weakly bound, multiply charged complexes of cucurbit[n]uril host molecules with alkali metal cations (Figure 1) provide an opportunity for studying this approach.

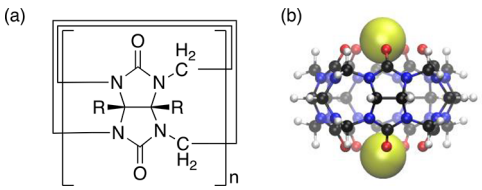

Figure 1. (a) Skeletal formula of cucurbit[n]uril (CB[n]). R = H for CB[5], CB[6], and CB[7] and R = CH_3 for decamethylcucurbit[5]-uril (mc5). Cyclohexanocucurbit[5]uril (CB*[5]) has the two R groups connected to each other, forming a 6-membered ring. (b) Complex of CB[5] with two Na^+ ions.

Cucurbit[n]urils and their derivatives are macrocyclic molecular receptors built from the association of n glycoluril repeat units.[15] They have a hydrophobic inner cavity and two identical carbonyl-lined portals that allow them to readily form host−guest complexes.[16] The two electronegative portals represent two binding sites for cations; thus, these hosts often function as ditopic ligands. The structure of such a complex is illustrated in Figure 1. These hollow, pumpkin-shaped molecules have attracted interest in the field of supramolecular chemistry due to their potential applications in areas such as drug delivery or sensitive analytical assays.[17−21] Further, these relatively small, simple molecular containers can serve as prototypes for much larger, more complicated structures, such as the binding pockets of enzymes. We are interested in measuring collision cross sections for gas-phase cucurbit[n]uril complexes as a means of obtaining structural information and distinguishing between isomeric or conformational possibilities using very small amounts of sample.

Cucurbit[n]uril (CB[n], n = 5, 6, and 7), decamethylcucurbit[5]uril (mc5), and cyclohexanocucurbit[5]uril (CB*[5]) (Figure 1) complexes of alkali metal cations are ideal targets for probing the effects of binding energy on CRAFTI CCS measurements. Whereas the cations are strongly bound in the +1 complexes, Coulombic repulsion in the +2 complexes decreases the binding strength of the second alkali metal cation[22] to levels that make dissociation relatively easy despite the fact that the ion is relatively massive compared to the neutral collision gas. Further, because the ligands are relatively rigid, we would expect the +1 and +2 complexes to have similar physical sizes.

In this study, we measure collision cross sections of CB[5], mc5, CB*[5], CB[6], and CB[7] complexed with alkali metal ions using both IM-MS and the "multi-CRAFTI"[23] technique (multi-CRAFTI is a method that performs CRAFTI on two or more ions at the same time, under identical pressure conditions at nearly identical center-of-mass kinetic energies). We compare the results obtained using the two techniques, and also compare the experimental results with computational methods using density functional theory for geometry optimization coupled with cross section calculations.[24]

In particular, we are interested in any differences that might arise due to differences in dissociation energies rather than due to real differences in physical size. Although we usually observed mixed-metal complexes as well, here we focus on homometal complexes to simplify the discussion. We will show that relative CCS values from IM-MS and multi-CRAFTI reflect the differences in intermolecular interactions that dominate under low- (in the case of drift IM-MS) vs high-energy (in the case of CRAFTI) collision conditions.

EXPERIMENTAL SECTION

Sample Preparation. CB[5], CB[6], CB[7], and all alkali metal salts are commercially available at Sigma-Aldrich (St. Louis, MO). A sample of mc5 was acquired from IBC Advanced Technologies (American Fork, Utah). CB*[5][25] was provided by Professor Kimoon Kim. ESI low concentration tune mix was obtained from Agilent Technologies (Santa Clara, CA). Ar and SF_6, which were used as collision gases in FTICR, and N_2, used as buffer gas in IM-MS (99.9997%, 99.8%, 99.999% purity, respectively), were purchased from Airgas, Inc. (Radnor, PA).

All solutions were prepared with cucurbit[n]uril host concentrations of 100 μM and an alkali salt concentration equal to twice that of the cucurbituril, in 1:1 2-propanol/water. These solutions were electrosprayed directly for multi-CRAFTI and diluted to a final concentration of about 20 μM in host to be used in IM-MS. Tune mix (specifically, Agilent standard m/z 922 with CCS of 243.64 ± 0.30 Å^2)[26] was added to all the IM-MS samples for calibration of the CCS. HPLC-grade solvents were used for all solutions. All of the solvents, cucurbituril complexes, and alkali metal salts were used as supplied without further purification.

FTICR Instrumentation. A Bruker model APEX 47e Fourier transform ion cyclotron resonance mass spectrometer with an Infinity trapping cell,[27,28] a microelectrospray source modified from an Analytica (Branford, CT, USA) design, and a metal capillary drying tube based on the design of Eyler et al.[29] was used in our experiments. Data were acquired using a MIDAS Predator data station.[30] The excitation clock rate was 5 MHz. Ions of interest were isolated using stored waveform inverse Fourier transform (SWIFT) techniques.[31] Ar or SF_6 collision gases were introduced into the FTICR cell using a Freiser-type pulsed leak valve.[32] Some multi-CRAFTI experiments were performed using both gases for comparison, but all systems were examined in SF_6 because it enables higher center-of-mass kinetic energy without ejecting the ions from the trapping cell. The pressure inside the cell was controlled by varying the duration of the leak valve pressurization event. Relative pressures in the cell were determined using a cold cathode pressure transducer. Collision energies were varied by changing the peak-to-peak amplitude of the excitation event at

https://doi.org/10.1021/jasms.2c00112
J. Am. Soc. Mass Spectrom. 2022, 33, 1644−1652

Table 1. Collision Cross-Section Ratios from Calculations and Experiments for Alkali Cation Complexes of Cucurbit[n]uril (CB[n], n = 5−7), mc5, and CB*[5] with Neutral Collision Gases As Indicated in Parentheses

		CCS(host+2M)$^{2+}$/ CCS(host+M)$^{+}$			
host, metal (M)	masses (+1, +2), Da	PA (SF_6)[a]	multi-CRAFTI (SF_6)[b]	TM (N_2)	IM-MS (N_2)
CB[5], Li	837.3, 844.3	0.98	[c]	1.10	1.11 ± 0.003
CB[5], Na	853.2, 876.2	0.99	0.95 ± 0.02	1.10	1.12 ± 0.007
CB[5], K	869.2, 908.2	1.01	1.04 ± 0.02	1.10	1.12 ± 0.002
CB[5], Rb	915.2, 1000.1	1.03	1.04 ± 0.02	1.10	1.11 ± 0.001
CB[5], Cs	963.2, 1096.1	1.05	1.05 ± 0.01	1.10	1.12 ± 0.001
mc5, Li	977.4, 984.4	0.99	[c]	1.09	1.10 ± 0.004
mc5, Na	993.4, 1016.4	0.99	0.94 ± 0.02	1.09	1.10 ± 0.002
mc5, K	1009.4, 1048.3	1.01	0.99 ± 0.03	1.08	1.09 ± 0.003
mc5, Rb	1055.3, 1140.2	1.04	1.03 ± 0.02	1.08	1.09 ± 0.004
mc5, Cs	1103.3, 1236.2	1.05	1.05 ± 0.01	1.08	1.09 ± 0.004
CB*[5], Na	1123.5, 1146.5	0.99	0.96 ± 0.02	1.08	1.09 ± 0.002
CB*[5], Cs	1233.4, 1366.3	1.03	1.00 ± 0.01	1.08	1.10 ± 0.002
CB[6], Na	1019.3, 1042.3	0.99	0.98 ± 0.01	1.08	1.10 ± 0.007
CB[6], Cs	1129.2, 1262.1	1.02	1.01 ± 0.01	1.08	1.10 ± 0.006
CB[7], Na	1185.3, 1208.3	0.99	0.98 ± 0.01	1.07	1.09 ± 0.009
CB[7], Cs	1295.2, 1428.2	1.02	[c]	1.07	1.09 ± 0.005

[a]Boltzmann-weighted averages from MMFF94 conformational searches to generate structures and energies and IMoS projected area approximation calculation for collision cross sections with SF_6. [b]Average ± standard deviation for ratios measured at the three highest center-of-mass kinetic energies in SF_6 collision gas. [c]Complex not detected experimentally.

the resonant frequencies of the ions of interest in multi-CRAFTI experiments. The ions being compared in multi-CRAFTI experiments were excited to nearly identical collision energies in the center-of-mass reference frame. We used summed single-frequency waveforms of identical duration (typically 0.5 ms, with relative amplitudes adjusted to produce the same center-of-mass collision energies E_{CM} with the neutral molecules according to eq 1[33]), yielding a simultaneous dual-frequency excitation. These waveforms were synthesized via a LabVIEW program.

$$E_{CM} = \frac{\beta^2 q^2 V_{pp}^2 t_{exc}^2}{8 d^2 m} \frac{M}{M+m} \quad (1)$$

In this equation, β is an instrument-dependent scaling factor (0.897 for the Infinity cell used here[28]), q is the ion charge, V_{PP} is the peak-to-peak excitation amplitude, t_{exc} is the duration of the excitation, d is the trapping cell diameter, and m and M are the masses of the ion and neutral, respectively. Data were analyzed using the Igor Pro software package (version 7, Wavemetrics Inc.; Lake Oswego, OR) to collect a set of power spectra measured at various collision gas pressures at each collision energy for each of the ion pairs. The collision cross section ratio of the two ions ($\frac{CCS_2}{CCS_1}$) (where CCS_1 = singly charged ion, and CCS_2 = doubly charged ion) was determined from the fwhm line widths of the ions using eq 2:[23]

$$\frac{CCS_2}{CCS_1} = \frac{fwhm_2}{fwhm_1} \frac{m_2 z_1}{m_1 z_2} \frac{V_{PP,1} t_{exc,1}}{V_{PP,2} t_{exc,2}} \quad (2)$$

Here $fwhm_n$ is the full width at half-maximum line width acquired using Lorentzian fits to the mass spectral data,[13] z_n is the ion charge, and the excitation durations for the two ions, $t_{exc,\,n}$, are the same, so that the $t_{exc,\,n}$ terms cancel. V_{pp} is the peak-to-peak amplitude of the excitation waveform at the frequency of interest, and m_n is the mass of the ion.

IM-MS Instrumentation. An Agilent 6560 Ion Mobility Quadrupole Time-of-Flight (IM-QTOF) device operated under uniform low field conditions was used to measure mobilities and corresponding CCS values of the ions. An Agilent nanoelectrospray ionization source (G1992A) was used to generate the ions. The IM-QTOF consists of a front funnel that runs at high pressure (4−4.50 Torr), a trap funnel and trapping gate that store and then release discrete packets of ions, a drift tube (~80 cm long) that separates ions based on their mobility, and a rear funnel that refocuses the ions before they enter a hexapole and are transmitted to the Q-TOF mass analyzer.[34] The front funnel and trap funnel were operated at 200 V peak-to-peak, and the rear ion funnel was operated at 100 V peak-to-peak (except for the case of CB[7], which was set to 200 V) . A fill time of 30,000 μs and release time of 300 μs were applied to the trap funnel.

The instrument provides drift time (t_d) information for ions. The Agilent IM-MS Browser software then calibrates and corrects the t_d information from the stepped-field measurements[35] and converts this to collision cross section using the Mason−Schamp equation.[7]

Computational Modeling. Modeling provides structural and energetic data to be compared with experimental data. We began with a Monte Carlo conformation search using the Merck molecular force field (MMFF94)[36] within the Spartan'18 software package (Wavefunction, Inc., Irvine, CA). Since MMFF94 does not include parameters for rubidium and cesium, user-selected parameters for those ions were inserted into the force field.[37] For cucurbit[n]uril and derivatives, the number of structures that need to be considered is relatively small because the host molecules are rigid. We used Spartan's Monte Carlo search algorithm to generate starting structures.

Once low energy conformers were identified, geometry optimizations on the lowest energy conformers for each host·cation system were performed at the B3LYP/6-311+G** level of theory to obtain final structures and energies, enabling host·cation binding energies to be determined. We report energies at 0 K, without counterpoise or vibrational corrections. Since the 6-311+G** basis set does not include parameters for

https://doi.org/10.1021/jasms.2c00112
J. Am. Soc. Mass Spectrom. 2022, 33, 1644−1652

rubidium and cesium, Spartan '18 defaults to a split basis set with def2-TZPPD (with pseudopotential) applied to rubidium and cesium.

IMoS[24,38] version 1.10c was used to compute collision cross sections from the theoretical structures. Either the very simple projection approximation (PA) or the somewhat more sophisticated exact hard-sphere scattering (EHSS)[39] method could be used to compute CCS values from calculated molecular structures for comparison with CRAFTI. The differences between PA and EHSS results for a given structure are small and comparable to the inherent error in the experimental measurements.[13] Because the PA method is computationally inexpensive compared to EHSS and models the single-collision dephasing conditions expected in CRAFTI, we opted to use the simple PA approach but would expect very similar results with EHSS. We therefore used PA with Ar and SF_6 collision gases to model CRAFTI, and used the trajectory method (TM)[9] with N_2 as the buffer gas for comparison and for modeling IM-MS. For the TM calculations, nitrogen's quadrupole moment was included, along with host·guest partial charges assigned using electrostatic potential (ESP) charges from the *ab initio* calculations.[40,41]

RESULTS

Multi-CRAFTI experiments directly yield ratios of CCS values for the ions being compared. Because relative CCS values are the focus here, we report all results in terms of ratios in the form $CCS[host+2M]^{2+}/CCS[host+M]^{+}$. Absolute CCS values can be obtained by comparison with standards of known CCS[23] (and are reported in the Supporting Information), but are not required for the comparisons that follow.

Computational Results. In the projection approximation (PA) calculations, all of the complexes of a given host have similar CCS values, and CCS values increase with increasing host size. Examining ratios (Table 1), doubly charged complexes have cross sections about 1−5% larger than their singly charged counterparts, except in the case of Li^+ and Na^+, for which the doubly charged complexes are 1−2% *smaller* than the corresponding singly charged complexes. In contrast, TM calculations for doubly charged complexes consistently yield collision cross sections 7−10% larger than their singly charged counterparts. For a given metal, as the host is varied the CCS +2/+1 ratio decreases as the size of the host increases, as expected given that the cross sections increasingly depend on the size of the host rather than on the metal.

Computational results for binding energies are shown in Table 2, without counterpoise or vibrational corrections, which would be small compared with the observed large differences between binding of the first and second cation to the complexes. Binding of an alkali cation to the neutral host is always significantly stronger (usually by a factor of 2 or more) than binding of a second cation to the singly charged (host +M)$^+$ complex, as expected due to significant Coulomb repulsion in the latter case.

Multi-CRAFTI Experimental Results. All the doubly and singly charged cucurbituril complex ions are easily observed in the electrospray mass spectra except for complexes of Li^+ ion and doubly charged complex of CB[7] with two Cs^+ ions. We performed multi-CRAFTI experiments in different collision gases (Ar and SF_6) for some of the complexes and obtained answers in decent agreement (Table S1). We report relative CCS in SF_6 collision gas in all the multi-CRAFTI experiments because SF_6 yields higher center-of-mass kinetic energy at any given ion orbit radius and thus is more likely to satisfy the energetic hard-sphere collision requirement[42] intrinsic to CRAFTI.

Table 2. Computed Binding Energies (B3LYP/6-311+G) of Cucurbituril Complexes**

host, metal (M)	D(CB[*n*]-M$^+$) (kJ/mol)	D(CB[*n*]M$^+$- M$^+$) (kJ/mol)
CB[5], Na	−404	−201
CB[5], K	−339	−144
CB[5], Rb	−309	−121
CB[5], Cs	−277	−99
mc5, Na	−437	−235
mc5, K	−367	−175
mc5, Rb	−361	−150
mc5, Cs	−300	−125
CB*[5], Na	−441	−243
CB*[5], Cs	−326	−145
CB[6], Na	−367	−179
CB[6], Cs	−285	−101
CB[7], Na	−405	−188
CB[7], Cs	−332	−34

Relative collision cross sections ($CCS[host+2M]^{2+}$/ $CCS[host+M]^{+}$, M = alkali metal) from multi-CRAFTI experiments are shown in Table 1 (absolute values are shown in Table S2). The multi-CRAFTI ratios involving the CB[5] host are shown in Figure 2 as a function of center-of-mass collision energy; the

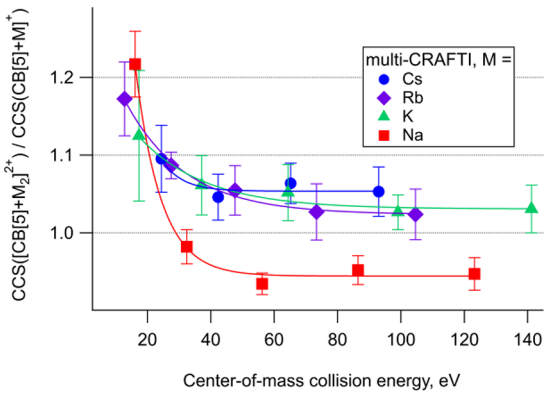

Figure 2. Multi-CRAFTI relative collision cross section ratio for doubly charged CB[5] complexes/singly charged complexes capped by various alkali metal cations. Error bars represent standard deviations for three or more replicate measurements, and lines are exponential fits to the experimental points.

results for other hosts are similar (Supporting Information, Figures S1−S4). In each case, the ratio decreases with collision energy until reaching a constant value at higher energies.

At the lowest energies (below 30−40 eV in the center-of-mass frame), the results are not reliable because the assumption of single-collision decoherence for both ions being compared, which is essential to CRAFTI,[12] is not valid. Because dissociation energies are lower for the +2 ions than for the corresponding +1 ions, collisions at these lower energies are more likely to dissociate the +2 ions and be "counted" as collisions than are similar interactions with +1 ions. Hence, the resulting ratios at low collision energies overemphasize CCS values for +2 ions and are larger than would be predicted from hard-sphere modeling.

At collision energies greater than about 35−40 eV for these complexes the multi-CRAFTI ratios become approximately

https://doi.org/10.1021/jasms.2c00112
J. Am. Soc. Mass Spectrom. 2022, 33, 1644−1652

constant as essentially all collisions result in dissociation for both +1 and +2 ions. Therefore, we concentrate on ratios at the high energy limit as accurate reflections of CCS ratios. The high-energy limiting value of $CCS[host+2M]^{2+}/CCS[host+M]^{+}$ is slightly less than 1 when M = Na, and is slightly greater than 1 for the larger alkali metal ions. These limiting values increase with the size of M in the order $Na^+ < K^+ \approx Rb^+ < Cs^+$, as expected based on the relative sizes of the alkali cations. We see the same trends for all other cucurbituril host complexes.

IM-MS Experimental Results. Collision cross section data for the various complex ions were measured by directly infusing them into the Agilent IM-MS instrument at seven different drift fields in N_2 buffer gas. The t_0 values for each complex were obtained from drift time vs 1/voltage graphs and then the corrected drift times (t_d) were used for CCS calculations. As shown in the last column of Table 1 (absolute values are shown in Table S2), the $CCS[host+2M]^{2+}/CCS[host+M]^{+}$ ratios from IM-MS for all examined hosts with different alkali metal ions are consistently greater than 1. Doubly charged complexes range between 9 and 12% larger than their singly charged counterpart complex ions, and are in excellent agreement with values computed using TM.

DISCUSSION

Effects of Binding Strength on CRAFTI Measurements. One of the original motivations for this study was to examine the influence of binding strength on CRAFTI measurements. We therefore compared CRAFTI cross sections for singly charged, relatively strongly bound complexes of the hosts and alkali metal ions with doubly charged, relatively weakly bound complexes.

Although m/z varies by nearly a factor of 2, the corresponding singly and doubly charged complexes of the same host should have similar physical sizes due to the rigidity of the host molecules. These expectations were generally borne out by our PA modeling results (Table 1), which indicate similar CCS values for +1 and +2 complexes. Interestingly, the model calculations predict that the +2 complexes of Li and Na should be a few percent smaller than the +1 complexes. We will address this further below.

In accordance with expectations, the modeling also shows that the singly charged complexes have much greater interaction energies than the corresponding doubly charged complexes (Table 2). Hence, if weaker binding yields larger apparent CRAFTI cross sections, we should observe the ratio $CCS(host+M_2)^{2+}/CCS(host+M)^{+}$ to be significantly greater than 1, especially where the difference in interaction energies is large. This is what we do observe at the lowest collision energies (below about 30 eV in Figure 2, for example). At higher collision energies, as both +1 and +2 ions dissociate on essentially every collision, the observed CCS ratio approaches a constant, high energy limit value, which we argue reflects the relative physical sizes of the molecules being compared. Thus, if binding interactions do not influence the high energy limit measurements significantly, for the complexes examined here we should observe $CCS(host+M_2)^{2+}/CCS(host+M)^{+}$ ratios near 1 that are consistent with the values from modeling. Examination of the high energy limit values reported in Table 1 shows experimental multi-CRAFTI ratios consistent with the computationally modeled PA results for all hosts.

When M = Na, the experimental ratio is significantly smaller than 1. While this is qualitatively consistent with the computational result, the experimental ratios are smaller than those computationally predicted, not larger as might be expected if interaction energy differences cause errors. Thus, we conclude that if interaction energy differences on the order of ~175—300 kJ mol^{-1} cause error in high energy limit CRAFTI cross section measurements, those errors are smaller than we can measure using current techniques.

Effects of Shifts in the Center-of-Mass. We note that both multi-CRAFTI and drift IM-MS CCS measurements involve rotational averaging and that a shift in the center-of-mass of the complex away from its geometric center could therefore affect the measured CCS ratios. The symmetric +2 complexes have mass uniformly distributed about the geometric center of the complex, whereas the +1 complexes have a guest ion on only one side, shifting the center-of-mass away from the geometric center and therefore possibly increasing the radius of rotation for the +1 ions. This should decrease the $CCS(host+M_2)^{2+}/CCS(host+M)^{+}$ ratio slightly (we estimate by 1−2%). Neither the PA nor the TM calculations take possible center-of-mass shifts into account, so comparison of the experimental results with the calculations might reveal possible center-of-mass effects. Comparison of multi-CRAFTI results with the PA calculations reveals that in almost all cases the experimentally measured $CCS(host+M_2)^{2+}/CCS(host+M)^{+}$ ratio is slightly smaller than that from the PA calculations, as would be expected if center-of-mass effects were skewing the results. However, the effect does not seem to become larger as the cation mass increases, as would be expected if center-of-mass shifts were the correct explanation. In contrast, the ratios from the IM-MS measurements are in every case slightly *larger* than those from the corresponding PA or TM calculations and are independent of alkali cation, so if center-of-mass effects are significant they do not show up at all in the IM-MS measurements. We conclude that neither the CRAFTI results nor the IM-MS results show obvious effects from shifts in the center-of-mass of the complexes.

Metal Size-dependent "Pinching" Effects in Cucurbituril Complexes Observed via Multi-CRAFTI. Our initial expectation was that perhaps the +2 complexes would have cross sections slightly larger than the +1 complexes because the +2 complexes have an additional surface atom, and Coulombic repulsion between the two metal ions might also stretch the complex somewhat. A perusal of the PA results in Table 1 shows that for M = Li or Na, $CCS(host+M_2)^{2+}/CCS(host+M)^{+}$ is less than 1 for all hosts, indicating the +2 complexes are computed to have collision cross sections a few percent smaller than those of the +1 complexes. The same is the case for the multi-CRAFTI measured cross sections involving M = Na, for all the hosts. In fact, for all hosts, the PA value of $CCS(host+M_2)^{2+}/CCS(host+M)^{+}$ increases monotonically with increasing metal size, and the experimental multi-CRAFTI values of the ratio are consistent with this trend.

What accounts for the Li^+ and Na^+ cases, which have +2 complexes that are smaller than the corresponding +1 complexes? As was noted above, one possibility is that shifts in the center-of-mass might account for this, but if so, center-of-mass effects should become more pronounced as the metal ions become heavier, and this is not observed. However, the results are consistent with a "pinching" effect when small metal ions bind in the portal of a cucurbituril host and attract the O atoms inward. To explore this idea, in Figure 3 we plot the change in the sum of O−O center-to-center distances around each portal of CB[5] as various alkali metal ions are added (as

https://doi.org/10.1021/jasms.2c00112
J. Am. Soc. Mass Spectrom. 2022, 33, 1644−1652

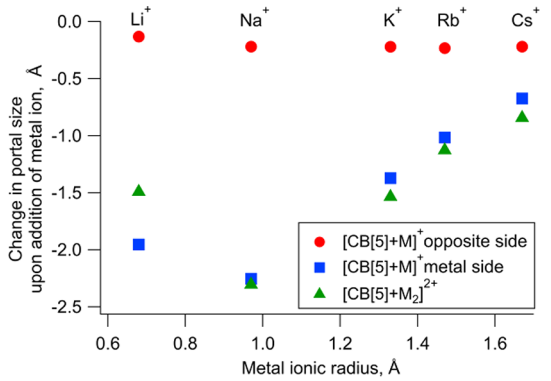

Figure 3. Change in portal circumference upon metal cation binding (as determined by summed O−O center-to-center distances around the portal) from B3LYP/6-31+G* calculations.

measured in structures from DFT theory) from the same sum in the free ligand. Not surprisingly, binding a metal ion in the portal of CB[5] causes the O−O circumferential distance to decrease as the positive metal ion pulls the electronegative oxygen atoms together, with Na^+ resulting in the most pinching of the portal and Cs^+ the least (Li^+ is too small to effectively interact with all 5 portal O atoms and distorts the portal shape, so while Li^+ does cause contraction, it has a smaller net effect than Na^+).

We initially expected that pinching one side of the ligand closer together might result in opening of the other portal, possibly accounting for the observed change in size of the +1 vs +2 complexes. The circles in Figure 3 report the change in portal size for the portal in the +1 complexes that does not contain a metal ion. The modeling results do not support the idea of the "opposite" side being pinched open. Rather, the O−O distances also decrease (relative to the free ligand) on the portal opposite that where the metal binds, although the changes are small and not strongly sensitive to the size of the metal ion. Pinching in the doubly charged complexes as measured via O−O distances (green triangles in Figure 3) is about the same on both portals as in the ion-bearing side of the singly charged complexes (blue squares in Figure 3) and again is greatest for the smallest metal ions. Pinching both portals in the +2 complexes causes a decrease in collision cross section, which is offset by the increases due to more surface atoms and Coulombic repulsion noted above. For the smallest alkali metal cations, the pinching on both sides of the +2 complexes is sufficient to make the +2 complexes have smaller CRAFTI cross sections than the corresponding +1 complexes, which are pinched on only one side. These changes are subtle but reproducible, consistent with modeling, and observed for every cucurbituril host we examined. This suggests that multi-CRAFTI cross section measurements can reveal structural changes that are relatively subtle.

Multi-CRAFTI Results Reflect Hard-Sphere Collisions; IM-MS Results Reflect Long-Range Interactions. We recognize that the neutral gas used in the CCS measurements plays a crucial role, and the best comparisons between CRAFTI and IM-MS could be made using the same neutral gas for both types of experiment. Unfortunately, such a direct comparison was not practical. One of the key conditions for CRAFTI experiments is that collisions occur in the energetic hard sphere limit,[42] where ions are lost in single collisions from the coherently orbiting packet prepared via resonant excitation. The preferred way to ensure single-collision decoherence is to conduct the experiments at collision energies high enough that the ions dissociate on virtually every collision. For the ions studied here, center-of-mass collision energies greater than about 30 eV are required to meet this condition. To achieve these collision energies for ions such as the cucurbituril complexes, relatively heavy neutral gases must be used (see eq 2). We have previously examined the effects of collision gases on CRAFTI results[11] and found that Ar and SF_6 can both yield satisfactory data for CB[n] complexes, although especially for the singly charged complexes the higher energies accessible using SF_6 are beneficial. Thus, SF_6 was the best collision gas for CRAFTI experiments. We did not use SF_6 in the IM-MS experiments because the continuous flow and long equilibration requirements of IM-MS mean that large amounts must be used. This was impractical with an expensive gas such as SF_6.

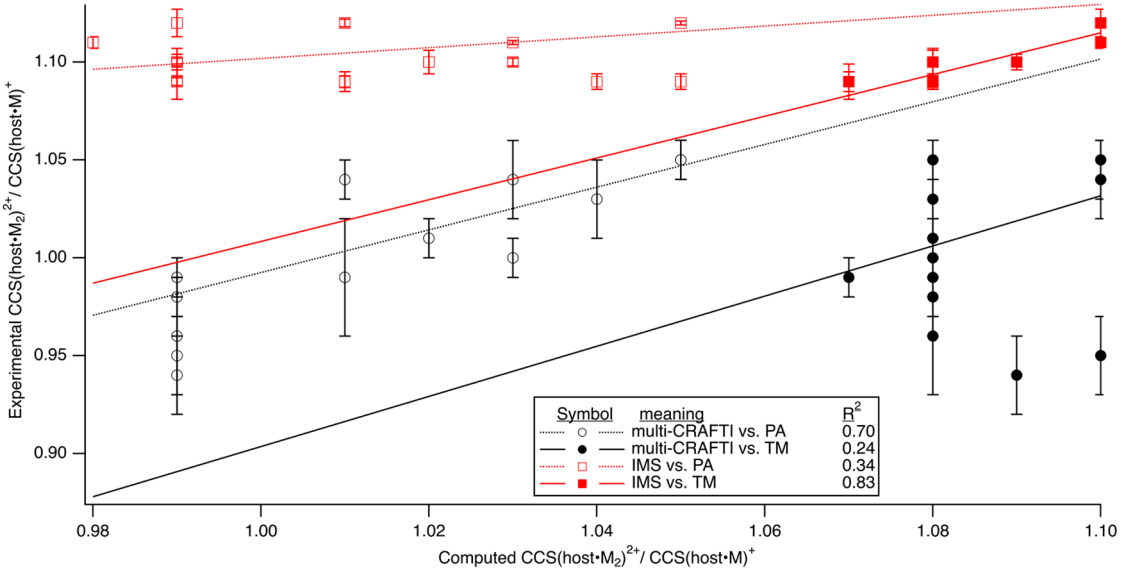

Figure 4. Relative collision cross section comparison of IM-MS, CRAFTI, TM, and PA methods. Error bars represent standard errors from IM-MS measurements and standard deviations from three or more replicate CRAFTI measurements.

https://doi.org/10.1021/jasms.2c00112
J. Am. Soc. Mass Spectrom. 2022, 33, 1644−1652

Hence, CRAFTI experiments on the FTICR were done in SF_6 (and to a limited extent in Ar), but IM-MS experiments were done in N_2. To mitigate the differences between the collision gases, we used internal standards in all experiments and report the ratios of cross sections measured against these internal standards. In addition, we note that the polarizabilities of N_2 (1.710 Å^3)[43] and Ar (1.664 Å^3)[43] are similar, whereas that of SF_6 (4.490 Å^3)[44] is much greater. The effects of long-range interactions should therefore be significantly greater in SF_6 than in N_2 (or Ar), whereas despite this we will show that CRAFTI experiments in highly polarizable SF_6 are more consistent with hard-sphere interactions than are IM-MS results in less polarizable N_2.

Relative CCS ratios obtained from multi-CRAFTI and IM-MS for singly- vs doubly charged complexes are clearly different (Table 1). Multi-CRAFTI results appear to correlate best with CCS values obtained using PA calculations from the model structures, whereas IM-MS measurements correlate better with CCS values from TM calculations on the same model structures. Figure 4 plots experimental measurements using multi-CRAFTI and IM-MS vs computed CCS values using PA and TM calculations for the same computed structures to show these correlations. We note that perfect agreement between theory and experiment in such a plot would yield a slope of 1, intercept of 0, and $R^2 = 1$. The plot of multi-CRAFTI vs PA has a slope of 1.1 ± 0.2 and intercept of −0.1 ± 0.2, with $R^2 = 0.70$, whereas plotting multi-CRAFTI vs TM yields slope 1.3 ± 0.3, intercept −0.4 ± 0.4, and $R^2 = 0.24$ (a much worse correlation). Similarly, plotting IM-MS CCS vs those calculated using TM gives slope = 1.1 ± 0.1, intercept −0.1 ± 0.1, and $R^2 = 0.83$, while plotting IM-MS vs PA gives slope 0.28 ± 0.02, intercept 0.83 ± 0.02, and $R^2 = 0.34$ (a much poorer correlation). In summary, the multi-CRAFTI measurements are more consistent with the PA calculations and show trends of increasing ratios as the sizes of the metal cations increase—they are sensitive to changes in CCS arising from changes in metal ion. The relative IM-MS experimental CCS measurements are in excellent agreement with values computed using TM but show little variation with metal ion, perhaps because long-range interactions smooth out those differences.

An increase of 9−12% in CCS for +2 over +1 complexes is consistent with a much larger role for long-range interactions in IM-MS measurements as compared with multi- CRAFTI. Long-range interactions depend strongly on the charge of the ion and the polarizability of the neutral, and are much more important at low collision velocities than at high collision velocities.[10,45] IM-MS measurements are deliberately carried out with low drift fields and low (close to thermal) ion-neutral collision energies and corresponding low velocities, where long-range interactions are expected to be important. In contrast, to satisfy the requirement that ion decoherence occurs in single collisions,[11−13,46] multi-CRAFTI is performed at much higher energies (typically tens to hundreds of eV in the center-of-mass reference frame) and correspondingly high relative velocities where long-range interactions are much less important, and collision cross sections are expected to be more accurately modeled via hard-sphere interactions.[10,45] Therefore, even though the IM-MS measurements were done in N_2, which is much less polarizable than the SF_6 used in the multi-CRAFTI measurements, long-range interactions are much more important in our IM-MS measurements than in our multi-CRAFTI measurements.

CONCLUSIONS

We explored the differences between the collision cross sections of the singly and doubly charged metal-cationized complexes of rigid host cucurbituril molecules that have similar physical sizes but quite different binding energies using both multi-CRAFTI and IM-MS techniques. The experimental data suggest that binding energy does not affect the CRAFTI cross section measurements noticeably, as long as the single-collision decoherence requirement is met.

The results of the current study also demonstrate theoretically expected differences between multi-CRAFTI and IM-MS measurements. Collision cross sections from multi-CRAFTI experiments tend to reflect hard-sphere interactions, which may allow probing of subtle differences in the physical sizes of the molecules that are more difficult to study using IM-MS experiments where long-range potentials play a larger role.

An example is found in the results presented here. The multi-CRAFTI measurements suggest small alkali cations pinch the portals of the hosts closed, causing smaller cross sections for the doubly charged ions than are observed for singly charged complexes of the same small alkali cation on CB[5] or mc5. Larger cations do not pull the CB[n] portal as tightly closed and protrude more, resulting in larger physical sizes for the doubly charged ions. The multi-CRAFTI measurements are sufficiently sensitive to observe subtle structural effects such as these, whereas our IM-MS measurements show very little variation as the metal ions vary, perhaps because these small effects are masked by long-range interactions. Interestingly, we note recent trapped ion mobility-time-of-flight (TIMS-TOF) measurements that did successfully measure differences due to the different sizes of lanthanide ions,[47] so at least in some cases mobility measurements at sufficiently high mobility resolution are able to detect these types of subtle structural effects.

ASSOCIATED CONTENT

Supporting Information

The Supporting Information is available free of charge at https://pubs.acs.org/doi/10.1021/jasms.2c00112.

Multi-CRAFTI data for singly- and doubly- charged CB[5] with Na and Cs ions in Ar and SF_6 (Table S1), collision cross sections of all cucurbit[n]uril CB[n] (n = 5−7) and derivative complex ions using multi-CRAFTI and PA (Table S2), collision cross sections of all cucurbit[n]uril CB[n] (n = 5−7) and derivative complex ions obtained from IM-MS experiments and trajectory method calculations (Table S3), multi-CRAFTI relative collision cross section ratios for doubly charged CB[n] (n = 6,7) and derivative complex ions/singly charged complexes (Figures S1−S4), representative mass spectrum of CB[5] electrosprayed from methanol/water solvent (Figure S5) (PDF)

AUTHOR INFORMATION

Corresponding Author

David V. Dearden − *Department of Chemistry and Biochemistry, Brigham Young University, Provo, Utah 84602-1030, United States;* orcid.org/0000-0003-0899-7776; Phone: +1 (801) 422-2355; Email: dvd@chem.byu.edu; Fax: +1 (801) 422-0153

https://doi.org/10.1021/jasms.2c00112
J. Am. Soc. Mass Spectrom. 2022, 33, 1644−1652

Authors

Tina Heravi − *Department of Chemistry and Biochemistry, Brigham Young University, Provo, Utah 84602-1030, United States*

Andrew J. Arslanian − *Department of Chemistry and Biochemistry, Brigham Young University, Provo, Utah 84602-1030, United States;* orcid.org/0000-0003-1622-5418

Spencer D. Johnson − *Department of Chemistry and Biochemistry, Brigham Young University, Provo, Utah 84602-1030, United States*

Complete contact information is available at: https://pubs.acs.org/10.1021/jasms.2c00112

Author Contributions

The manuscript was written through contributions of all authors.

Notes

The authors declare no competing financial interest.

■ ACKNOWLEDGMENTS

The authors thank the National Science Foundation for financial support (CHE-1904838). We are also grateful to Professor Kimoon Kim and his research group at the Pohang University of Science and Technology for providing a sample of CB*[5]. S.D.J. thanks BYU's College of Physical and Mathematical Sciences for undergraduate research funds. A.J.A. also thanks the Roland K. Robins, Rex and Marcia A. Goates, and the Loren and Maurine F. Bryner families for graciously funding graduate research fellowships awarded to him by BYU's Department of Chemistry and Biochemistry.

■ REFERENCES

(1) Lanucara, F.; Holman, S. W.; Gray, C. J.; Eyers, C. E. The power of ion mobility-mass spectrometry for structural characterization and the study of conformational dynamics. *Nat. Chem.* **2014**, *6*, 281−294.

(2) Lee, J. W.; Lee, H. H.; Ko, Y. H.; Kim, K.; Kim, H. I. Deciphering the specific high-affinity binding of cucurbit[7]uril to amino acids in water. *J. Phys. Chem. B* **2015**, *119*, 4628−4636.

(3) Choi, T. S.; Ko, J. Y.; Heo, S. W.; Ko, Y. H.; Kim, K.; Kim, H. I. Unusual Complex Formation and Chemical Reaction of Haloacetate Anion on the Exterior Surface of Cucurbit[6]uril in the Gas Phase. *J. Am. Soc. Mass Spectrom.* **2012**, *23*, 1786−1793.

(4) Kalenius, E.; Groessl, M.; Rissanen, K. Ion mobility−mass spectrometry of supramolecular complexes and assemblies. *Nat. Rev. Chem.* **2019**, *3*, 4−14.

(5) Clemmer, D. E.; Hudgins, R. R.; Jarrold, M. F. Naked protein conformations: cytochrome c in the gas phase. *J. Am. Chem. Soc.* **1995**, *117*, 10141−10142.

(6) Eiceman, G. A.; Karpas, Z.; Hill, H. H., Jr *Ion mobility spectrometry*; CRC Press, 2013.

(7) Revercomb, H. E.; Mason, E. A. Theory of Plasma Chromatography Gaseous Electrophoresis - Review. *Anal. Chem.* **1975**, *47*, 970−983.

(8) Merenbloom, S. I.; Flick, T. G.; Williams, E. R. How hot are your ions in TWAVE ion mobility spectrometry? *J. Am. Soc. Mass Spectrom.* **2012**, *23*, 553−562.

(9) Mesleh, M. F.; Hunter, J. M.; Shvartsburg, A. A.; Schatz, G. C.; Jarrold, M. F. Structural Information from Ion Mobility Measurements: Effects of the Long-Range Potential. *J. Phys. Chem.* **1996**, *100*, 16082−16086.

(10) Shirts, R. B. Collision Theory and Reaction Dynamics. In *Gaseous Ion Chemistry and Mass Spectrometry*; Futrell, J. H., Ed.; John Wiley & Sons, 1986; pp 25−57.

(11) Yang, F.; Jones, C. A.; Dearden, D. V. Effects of Kinetic Energy and Collision Gas on Measurement of Cross Sections by Fourier Transform Ion Cyclotron Resonance Mass Spectrometry. *Int. J. Mass Spectrom.* **2015**, *378*, 143−150.

(12) Yang, F.; Voelkel, J. E.; Dearden, D. V. Collision Cross Sectional Areas from Analysis of Fourier Transform Ion Cyclotron Resonance Line Width: A New Method for Characterizing Molecular Structure. *Anal. Chem.* **2012**, *84*, 4851−4857.

(13) Anupriya; Gustafson, E.; Mortensen, D. N.; Dearden, D. V. Quantitative Collision Cross-sections from FTICR Linewidth Measurments: Improvements in Theory and Experiment. *J. Am. Soc. Mass Spectrom.* **2018**, *29*, 251−259.

(14) Heravi, T.; Shen, J.; Johnson, S.; Asplund, M. C.; Dearden, D. V. Halide Size-Selective Binding by Cucurbit[5]uril—Alkali Cation Complexes in the Gas Phase. *J. Phys. Chem. A* **2021**, *125*, 7803−7812.

(15) Mock, W. L.; Shih, N. Y. Dynamics of Molecular Recognition Involving Cucurbituril. *J. Am. Chem. Soc.* **1989**, *111*, 2697−2699.

(16) Wittenberg, J. B.; Zavalij, P. Y.; Isaacs, L. Supramolecular ladders from dimeric cucurbit[6]uril. *Angew. Chem., Int. Ed. Engl.* **2013**, *52*, 3690−3694.

(17) Jin Jeon, Y.; Kim, S.-Y.; Ho Ko, Y.; Sakamoto, S.; Yamaguchi, K.; Kim, K. Novel molecular drug carrier: encapsulation of oxaliplatin in cucurbit[7]uril and its effects on stability and reactivity of the drug. *Org. Biomol. Chem.* **2005**, *3*, 2122−2125.

(18) Bali, M. S.; Buck, D. P.; Coe, A. J.; Day, A. I.; Collins, J. G. Cucurbituril binding of *trans*-[{PtCl $(NH_3)_2$}$_2$ (μ-$NH_2(CH_2)_8NH_2$)]$^{2+}$ and the effect on the reaction with cysteine. *Dalton Trans.* **2006**, 5337−5344.

(19) Kemp, S.; Wheate, N. J.; Wang, S. Y.; Collins, J. G.; Ralph, S. F.; Day, A. I.; Higgins, V. J.; Aldrich-Wright, J. R. Encapsulation of platinum(II)-based DNA intercalators within cucurbit[6,7,8]urils. *J. Biol. Inorg. Chem.* **2007**, *12*, 969−979.

(20) Wheate, N. J. Improving platinum(II)-based anticancer drug delivery using cucurbit[*n*]urils. *J. Inorg. Biochem.* **2008**, *102*, 2060−2066.

(21) Zhao, Y.; Bali, M. S.; Cullinane, C.; Day, A. I.; Collins, J. G. Synthesis, cytotoxicity and cucurbituril binding of triamine linked dinuclear platinum complexes. *Dalton Trans.* **2009**, 5190−5198.

(22) Mortensen, D. N.; Dearden, D. V. Influence of charge repulsion on binding strengths: experimental and computational characterization of mixed alkali metal complexes of decamethylcucurbit [5] uril in the gas phase. *Chem. Commun.* **2011**, *47*, 6081−6083.

(23) Pope, B. L.; Joaquin, D.; Hickey, J. T.; Mismash, N.; Heravi, T.; Shrestha, J.; Arslanian, A. J.; Anupriya; Mortensen, D. N.; Dearden, D. V. Multi-CRAFTI: Relative Collision Cross Sections from Fourier Transform Ion Cyclotron Resonance Mass Spectrometric Line Width Measurements. *J. Am. Soc. Mass Spectrom.* **2022**, *33*, 131−140.

(24) Shrivastav, V.; Nahin, M.; Hogan, C. J.; Larriba-Andaluz, C. Benchmark Comparison for a Multi-Processing Ion Mobility Calculator in the Free Molecular Regime. *J. Am. Soc. Mass Spectrom.* **2017**, *28*, 1540−1551.

(25) Zhao, J.; Kim, H.-J.; Oh, J.; Kim, S.-Y.; Lee, J. W.; Sakamoto, S.; Yamaguchi, K.; Kim, K. Cucurbit[*n*]uril Derivatives Soluble in Water and Organic Solvents. *Angew. Chem., Int. Ed.* **2001**, *40*, 4233−4235.

(26) Stow, S. M.; Causon, T. J.; Zheng, X.; Kurulugama, R. T.; Mairinger, T.; May, J. C.; Rennie, E. E.; Baker, E. S.; Smith, R. D.; McLean, J. A.; et al. An Interlaboratory Evaluation of Drift Tube Ion Mobility−Mass Spectrometry Collision Cross Section Measurements. *Anal. Chem.* **2017**, *89*, 9048−9055.

(27) Sievers, H. L.; Grützmacher, H.-F.; Caravatti, P. The geometrical factor of infinitely long cylindrical ICR cells for collision energy-resolved mass spectrometry: appearance energies of EI_2^+ (E= P, As, Sb, and Bi) from collision-induced dissociation of EI_3^+ and [EI_2·ligand]$^+$ complexes. *Int. J. Mass Spectrom. Ion Proc.* **1996**, *157*, 233−247.

(28) Caravatti, P.; Allemann, M. The 'infinity cell': A new trapped-ion cell with radiofrequency covered trapping electrodes for fourier transform ion cyclotron resonance mass spectrometry. *Org. Mass Spectrom.* **1991**, *26*, 514−518.

(29) Wigger, M.; Nawrocki, J. P.; Watson, C. H.; Eyler, J. R.; Benner, S. A. Assessing enzyme substrate specificity using combinatorial libraries and electrospray ionization-Fourier transform ion cyclotron resonance mass spectrometry. *Rapid Commun. Mass Spectrom.* **1997**, *11*, 1749−1752.
(30) Blakney, G. T.; Hendrickson, C. L.; Marshall, A. G. Predator data station: a fast data acquisition system for advanced FT-ICR MS experiments. *Int. J. Mass Spectrom.* **2011**, *306*, 246−252.
(31) Chen, L.; Wang, T. C. L.; Ricca, T. L.; Marshall, A. G. Phase-modulated stored waveform inverse Fourier transform excitation for trapped ion mass spectrometry. *Anal. Chem.* **1987**, *59*, 449−454.
(32) Jiao, C. Q.; Ranatunga, D. R. A.; Vaughn, W. E.; Freiser, B. S. A pulsed-leak valve for use with ion trapping mass spectrometers. *J. Am. Soc. Mass Spectrom.* **1996**, *7*, 118−122.
(33) Marshall, A. G.; Hendrickson, C. L.; Jackson, G. S. Fourier Transform Ion Cyclotron Resonance Mass Spectrometry: A Primer. *Mass Spectrom. Rev.* **1998**, *17*, 1−35.
(34) Kurulugama, R.; Imatani, K.; Taylor, L. The Agilent Ion Mobility Q-TOF Mass Spectrometer System. *Technical overview by Agilent Technologies* 2013, https://www.agilent.com/cs/library/technicaloverviews/public/5991-3244EN.pdf
(35) Cole, R. B. *Electrospray and MALDI mass spectrometry: fundamentals, instrumentation, practicalities, and biological applications*; John Wiley & Sons, 2011.
(36) Halgren, T. A. Merck molecular force field. I. Basis, form, scope, parameterization, and performance of MMFF94. *J. Comput. Chem.* **1996**, *17*, 490−519.
(37) Hickenlooper, S. M.; Harper, C. C.; Pope, B. L.; Mortensen, D. N.; Dearden, D. V. Barriers for Extrusion of a Guest from the Interior Binding Cavity of a Host: Gas Phase Experimental and Computational Results for Ion-Capped Decamethylcucurbit[5]uril Complexes. *J. Phys. Chem. A* **2018**, *122*, 9224−9232 research-article.
(38) Czerwinska, I.; Far, J.; Kune, C.; Larriba-Andaluz, C.; Delaude, L.; De Pauw, E. Structural analysis of ruthenium-arene complexes using ion mobility mass spectrometry, collision-induced dissociation, and DFT. *Dalton Trans.* **2016**, *45*, 6361−6370.
(39) Shvartsburg, A. A.; Jarrold, M. F. An exact hard-spheres scattering model for the mobilities of polyatomic ions. *Chem. Phys. Lett.* **1996**, *261*, 86−91.
(40) Breneman, C. M.; Wiberg, K. B. Determining atom-centered monopoles from molecular electrostatic potentials. The need for high sampling density in formamide conformational analysis. *J. Comput. Chem.* **1990**, *11*, 361−373.
(41) Besler, B. H.; Merz, K. M., Jr; Kollman, P. A. Atomic charges derived from semiempirical methods. *J. Comput. Chem.* **1990**, *11*, 431−439.
(42) Guo, D.; Xin, Y.; Li, D.; Xu, W. Collision cross section measurements for biomolecules within a high-resolution FT-ICR cell: theory. *Phys. Chem. Chem. Phys.* **2015**, *17*, 9060−9067.
(43) Olney, T. N.; Cann, N. M.; Cooper, G.; Brion, C. E. Absolute scale determination for photoabsorption spectra and the calculation of molecular properties using dipole sum-rules. *Chem. Phys.* **1997**, *223*, 59−98.
(44) Gussoni, M.; Rui, R.; Zerbi, G. Electronic and relaxation contribution to linear molecular polarizability. An analysis of the experimental values. *J. Mol. Struct.* **1998**, *447*, 163−215.
(45) Su, T.; Bowers, M. T. Classical Ion−Molecule Collision Theory. In *Gas Phase Ion Chemistry*; Bowers, M. T., Ed.; Academic, 1979; Vol. *1*, pp 83−118.
(46) Anupriya; Jones, C. A.; Dearden, D. V. Collision Cross Sections for 20 Protonated Amino Acids: Fourier Transform Ion Cyclotron Resonance and Ion Mobility Results. *J. Am. Soc. Mass Spectrom.* **2016**, *27*, 1366−1375.
(47) Schäfer, A.; Vetsova, V. A.; Schneider, E. K.; Kappes, M.; Seitz, M.; Daumann, L. J.; Weis, P. Ion Mobility Studies of Pyrroloquinoline Quinone Aza-Crown Ether−Lanthanide Complexes. *J. Am. Soc. Mass Spectrom.* **2022**, *33*, 722−730.

https://doi.org/10.1021/jasms.2c00112
J. Am. Soc. Mass Spectrom. 2022, 33, 1644−1652